Supplementary materials: Land-use change emissions based on high-resolution activity data substantially lower than previously estimated

R. Ganzenmüller[1,*], S. Bultan[1], K. Winkler[2,3], R. Fuchs[2], F. Zabel[1], and J. Pongratz[1,4]

[1]Department of Geography, Ludwig-Maximilians-Universität München, Munich, Germany
[2]Institute of Meteorology and Climate Research, Atmospheric Environmental Research (IMK-IFU), Karlsruhe Institute of Technology, Garmisch-Partenkirchen, Germany
[3]Department of Environmental Sciences, Wageningen University & Research (WUR), Wageningen, the Netherlands
[4]Max Planck Institute for Meteorology, Hamburg, Germany
[*]Contact: raphael.ganzenmueller@geographie.uni-muenchen.de

A Data and data processing

A.1 Data

Reconstructing global, long-term LULCC dynamics is a challenging task due to the lack of spatial and temporal details in historical documents and missing consistency. The most comprehensive historical land-use dataset on global scale is LUH2 (Chini et al. 2021; Hurtt et al. 2020). At a resolution of 0.25°x0.25°, it covers the years AD 850 to 2100 and provides information on multiple crop, pasture, and forest types and its management practices, such as shifting cultivation and wood harvest. The latest published version of LUH2 (Chini et al. 2021) is based on HYDE 3.2 (Klein Goldewijk et al. 2017), but also uses satellite information and other data streams such as FAO (2021), Hansen et al. (2013), and Zhang et al. (2015). Due to its comprehensiveness, long time span, and global coverage, LUH2 serves as input for CMIP6 simulations and the GCB assessments.

Other global LULCC datasets are covering only limited land use categories (HYDE (Klein Goldewijk et al. 2017), Millennium Reconstruction of cropland and pasture (Pongratz et al. 2008), SAGE cropland (Ramankutty and Foley 1999)) or are of limited temporal coverage (GLASS-GLC (Liu et al. 2020), ESA-CCI (ESA 2017), MODIS (Friedl et al. 2002)). Both aspects restrict the usability of these global datasets for E_{LUC} assessments.

The new LULCC dataset HILDA+ (Winkler et al. 2021) overcomes these limitations. HILDA+ has six land cover classes (urban, cropland, pasture/rangeland, forest, unmanaged grass/shrubland, sparse/no vegetation) and a temporal coverage of 1960–2019, with trends interpolated linearly back to 1900 based on the data-driven dynamics after 1960, and a spatial resolution of 0.01°x0.01°. It has a binary classification scheme and transitions between LULCC categories are reported fully as gross changes per grid cell, which separates HILDA+ from most other LULCC datasets. Gross changes consider only absolute changes, i.e., the state of one grid cell changes as a whole. In contrast, net changes also reflect sub-grid transitions. Gross and net LULCC transitions should not be confused with gross and net emission component fluxes. HILDA+ was generated by combining 21 global and regional data streams including remote sensing products, LULCC reconstructions and statistics. Further information on HILDA+ can be found in Winkler et al. (2021).

A.2 Processing of HILDA+

To be able to compare to earlier BLUE simulations and isolate the effect of only the LULCC forcing, we apply the same pre-processing to HILDA as we did to LUH2-based simulations; LULCC information is provided in the four classes cropland, pasture, secondary land, and primary land. Thus, we aggregated the HILDA+ classes urban and pasture/rangeland to one category (“pasture”) and forest, unmanaged grass/shrub land, sparse/no vegetation to another (“primary/secondary land”). Adding urban to the “pasture” class is in line with the implementation of LUH2 in BLUE. To split the “primary/secondary land” class, the respective forest and non-forest data was extracted for each year from LUH2 and regridded (method: “nearest neighbor”) from 0.25° to 0.01° resolution. Subsequently, for grid cells without transitions in former years the ratio of the regridded LUH2 primary and secondary land information was taken of each year to split the combined class of forest, unmanaged grass/shrub land, and sparse/no vegetation in separate “primary land” and “secondary land” categories. Grid cells that were cropland or pasture in HILDA+ in any year before were classified as secondary land.

A.3 LUH2 Harvest reallocation

Since HILDA+ does not provide data on wood harvest, this information had to be taken from LUH2. However, in addition to the different resolution, wood harvest in LUH2 often does not match suitable areas in HILDA+, i.e., wood harvest would be assigned to cropland or pasture. Thus, a reallocation scheme was developed to (a) allow wood harvest only on grid cells where it is actually possible and (b) preserve primary and secondary wood harvest areas of LUH2 in each country. The conservation of national wood harvest data is justified by original LUH2 wood harvest information being based on national statistics (Hurtt et al. 2020).

In a first step, LUH2 wood harvest was regridded (method: nearest neighbor) from 0.25° to 0.01° resolution. Second, the different LUH2 wood harvest types (wood harvest from secondary young forest land, from secondary mature forest land, secondary non-forest land, primary forest land, and primary non-forest land) were aggregated to the classes “harvest on primary land” and “harvest on secondary land”. Third, for each country, LUH2 primary and secondary harvest were reallocated from grid cells where HILDA+ locates cropland or pasture to grid cells where (a) HILDA+ locates primary or secondary land, (b) LUH2 already has primary or secondary harvest, and (c) the primary/secondary harvest area does not exceed primary/secondary land area. The reallocation from cells with a harvest mismatch to grid cells that fulfill above-mentioned criteria, is done proportionally in an iterative manner until the maximum aggregated mismatch in one year is less than 1 km^2 in the respective country. Finally, the reallocated primary and secondary harvest areas were split into the different LUH2 harvest types based on

the original ratios in each grid cell. In some countries, the aggregated primary or secondary harvest area of LUH2 temporarily exceeds the aggregated primary resp. secondary states area of HILDA+. In these cases, it is assumed that the harvest area corresponds with the respective state area.

B Data comparison: HILDA+ and LUH2

HILDA+ and LUH2 (as used in BLUE) differ in land cover states area, the annual change of land cover states and the spatial distribution of land cover categories (Figure S1, S2, S3). While globally total area and spatial distributions of cropland is fairly similar on global scale (difference of global total area averaged over 1960–2019: 3 %), larger differences exist for pasture, secondary land, and primary land (difference of global total area averaged over 1960–2019: 63 %, 14%, resp. 25 %). Moreover, the annual change of cropland and secondary land is far greater in LUH2, while the contrary is true for pasture. In the following, cropland and pasture values from FAOSTAT (FAO 2021) are used in addition for a better comparison.

Similar to the total cropland area, the spatial distribution differs only slightly on all continents, without extreme mismatches (Figure S3). Both HILDA+ and LUH2 cropland area totals between 1960 and 2019 are in the same range as FAOSTAT reported values (Figure S2). However, the increase in cropland area in LUH2 in most recent years is not reflected in HILDA+ and FAO (2021). Another big difference is the gross change of cropland with far larger values in LUH2 (Figure S1). The size of this difference, which can also be seen to some degree for secondary land, is connected to the implementation of shifting cultivation in LUH2 and the omission of it in HILDA+. In LUH2 shifting cultivation is added to transitions between cropland and natural vegetation (with a prioritization of secondary land) based on shifting cultivation occurrence rates derived from Heinimann et al. (2017) (Hurtt et al. 2020). The much higher gross gains and losses of cropland and secondary land in LUH2 are limited to tropical and subtropical regions with shifting cultivation, highlighted in Figure 4 and 5 in Heinimann et al. (2017).

The difference in pasture area between the two datasets is substantial, with global areas being about three times larger in HILDA+ and FAO (2021) compared to the LUH2 version used in BLUE. The larger pasture areas of HILDA+ are present on almost all continents, with the highest discrepancies occurring in grassland-dominated regions in Australia, Central Asia, Africa, and North America. Contrary to cropland and secondary land, the annual gross change of pasture is larger in HILDA+ compared to LUH2. The differences in pasture areas and annual changes originate in different pasture derivations and further processing steps of the underlying data: HILDA+ is based on the FAO category “permanent meadows and pastures” from 2019 and FAO livestock data (Winkler et al. 2021) and implicitly includes rangelands in the pasture category. On the contrary, LUH2 is derived from HYDE3.2 (Hurtt et al. 2020), which is based on the 2015 version of FAO “permanent meadows and pastures” values (Klein Goldewijk et al. 2017). The here shown values of LUH2 for pasture include rangelands only partially (processing of rangelands for BLUE according to Le Quéré et al. (2018, Tab. 4) using ancillary information from LUH2 to distinguish between pasture expansion transforming natural vegetation to grassland and grazing that leaves the general type of vegetation (e.g., forest or shrubland) unaltered).

As a logical consequence of the larger pasture areas in HILDA+, secondary and primary land areas are much larger in LUH2. The above-mentioned regions with larger pasture areas in HILDA+ are also the regions with larger areas of secondary and primary land in LUH2. Nevertheless, the annual net change of secondary land in HILDA+ is larger than in LUH2. In addition, the annual net change of secondary land in HILDA+ is positive in most years since 1970, while the one in LUH2 is negative in the last decade (as a result of the cropland expansion). Annual change rates of primary land are slightly more negative in HILDA+.

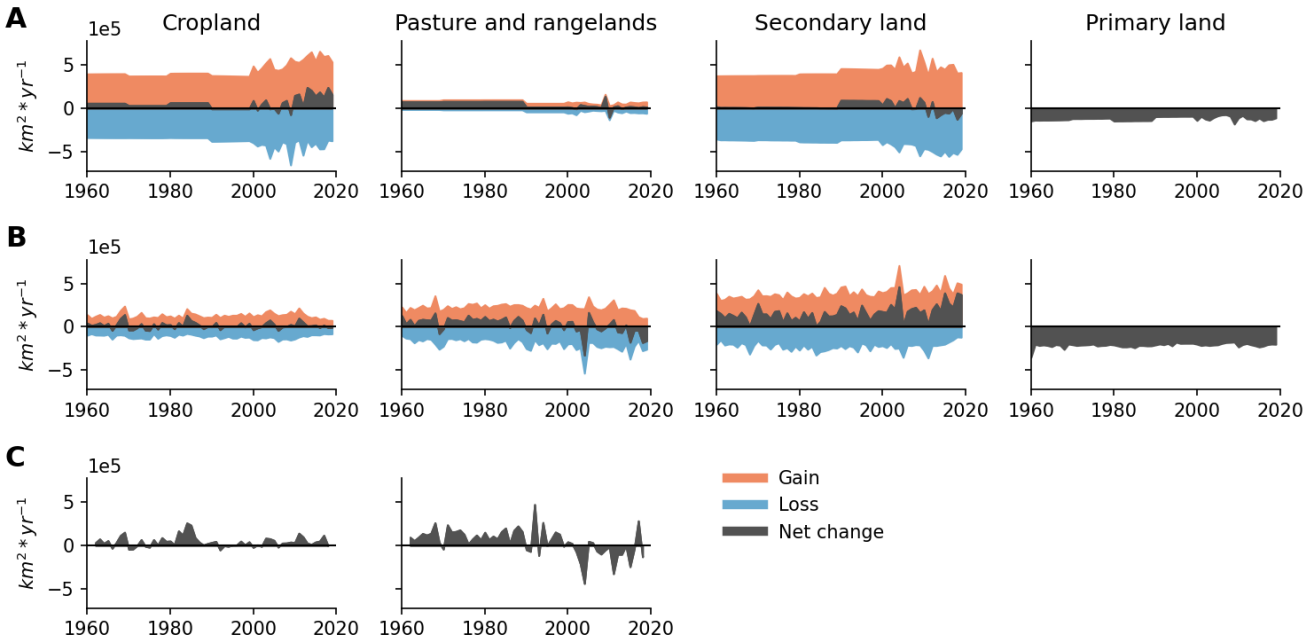

Figure S1. Global annual change of cropland, pasture and rangelands, secondary land and primary land. A: LUH2 (as used in BLUE), B: HILDA+ (as used in BLUE), C: FAOSTAT (from FAO (2021), statistics on primary and secondary land not reported). In HILDA+ pasture contains rangelands, while in the LUH2 version prepared for BLUE rangelands are partly attributed to pasture and partly to secondary land as described in Le Quéré et al. (2018, Tab. 4). Gross change of cropland and secondary land of LUH2 are a substantially higher compared to HILDA+, while for pasture it is the contrary. Furthermore, LUH2 net change of cropland increases in the last decade, whereas HILDA+ and FAO (2021) have a downward trend. FAO (2021) coincides in many years with the values from HILDA+. Figure S2 shows the time series for absolute states areas. Note: Annual change values of LUH2 from Figure 4 in Winkler et al. (2021) are based on the LUH2 states file instead of the transition files used here to capture all subgrid-scale transitions.

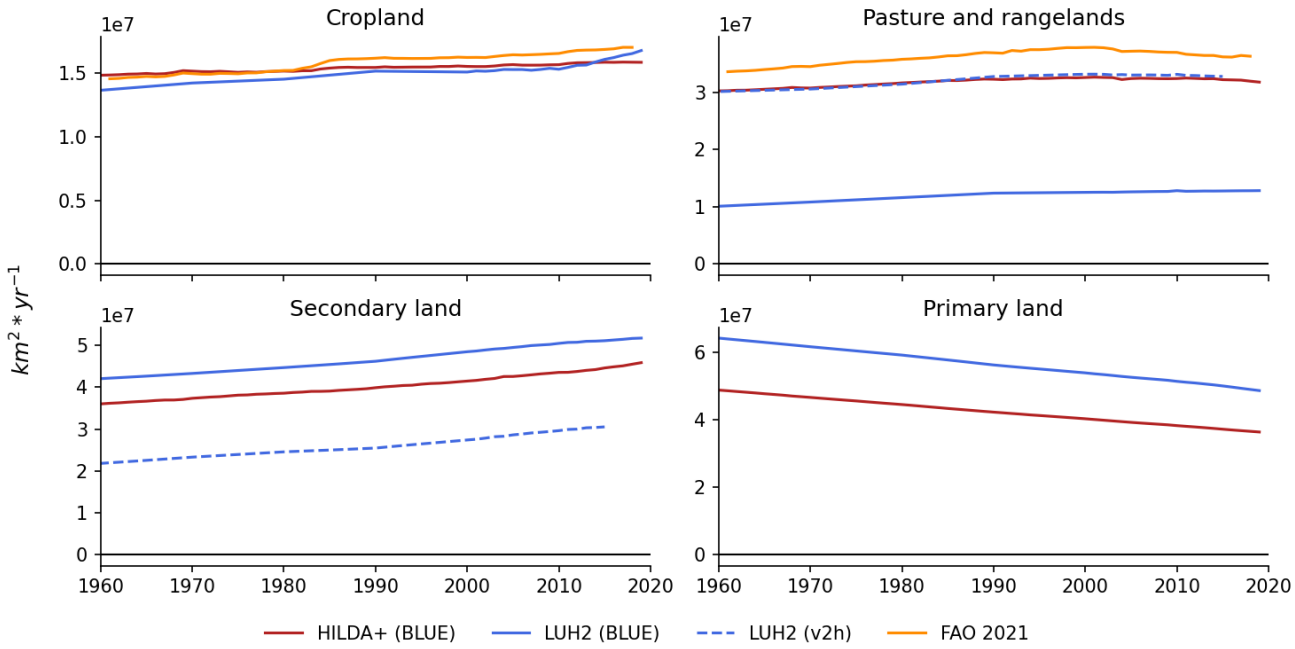

Figure S2. Global land-use and land-cover states of LUH2 and the reclassified and prepared HILDA+ dataset for 1960-2019. The original HILDA+ dataset has six LULCC classes and no distinction between primary and secondary land (see Sec. 2). In HILDA+ pasture contains rangelands, while in the LUH2 version prepared for BLUE rangelands are partly attributed to pasture and partly to secondary land as described in Le Quéré et al. (2018, Tab. 4) using ancillary information from LUH2 to distinguish between pasture expansion transforming natural vegetation to grassland and grazing that leaves the general type of vegetation (e.g., forest or shrubland) unaltered. "LUH2 (v2h)" shows the pasture (and secondary land) areas before this distinction is applied. Additionally, cropland and pasture area estimates of FAO (2021) are included for comparison. Estimates of cropland area are in the same range, whereas the pasture area from HILDA+ and (FAO 2021) are substantially higher than in LUH2. Consequently, secondary and primary land areas of LUH2 are larger than those for HILDA+.

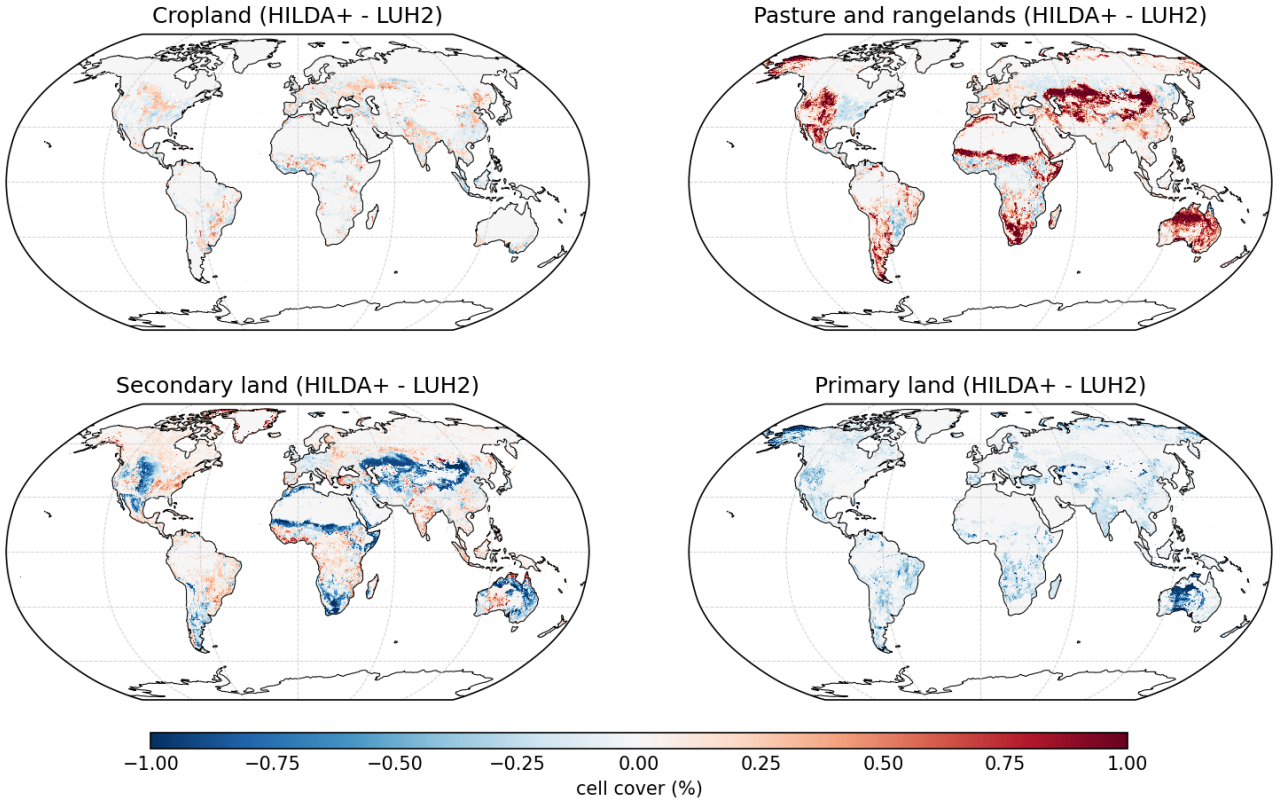

Figure S3. Difference in land-use and land-cover states areas of HILDA+ and LUH2 in 2010. Main differences exist for pasture and secondary land arid regions in North America, Africa, Central Asia and Oceania. The differences in cropland and primary land areas are comparably small.

C Regions

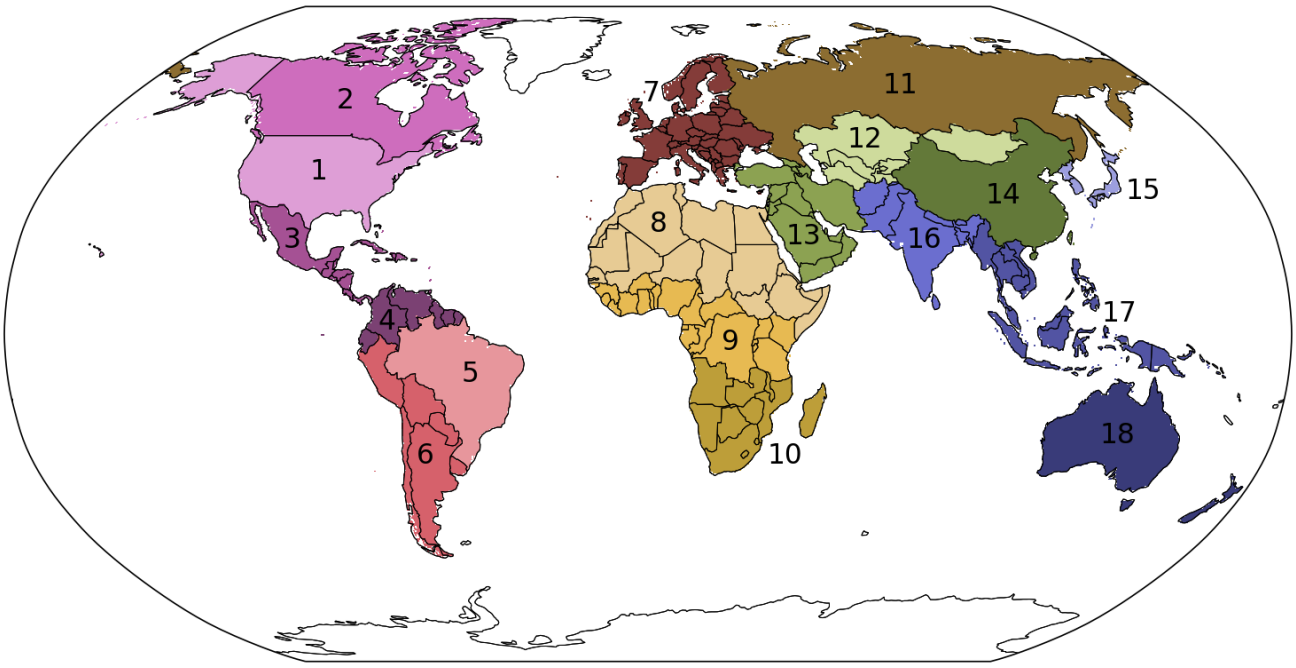

Figure S4. Region definitions used in this study (derived from the RECCAP-2 project): 1: USA; 2: Canada; 3: Central America; 4: Northern South America; 5: Brazil; 6: Southwest South America; 7: Europe; 8: Northern Africa; 9: Equatorial Africa; 10: Southern Africa; 11: Russia; 12: Central Asia; 13: Mideast; 14: China; 15: Korea and Japan; 16: South Asia; 17: Southeast Asia; 18: Oceania.

D Global and regional mean ELUC estimates of BLUE simulations based on HILDA+ at 0.25° and 0.01° resolution and LUH2

Table S1. Yearly mean E_{LUC} estimates of a BLUE simulation based on HILDA+ at 0.25° resolution, 1960-2019, TgC*yr^{-1}).

	E_{LUC}	E_{SINK}	E_{SOURCE}	E_{CROP}	$E_{PASTURE}$	$E_{HARVEST}$	$E_{ABANDONMENT}$
Global	1022	-1526	2548	793	299	644	-714
USA	-30	-130	101	44	25	-4	-94
Canada	61	-55	116	14	1	57	-11
Central America	56	-28	84	35	14	21	-14
Northern South America	33	-14	46	7	20	13	-7
Brazil	208	-47	255	66	83	73	-14
Southwest South America	73	-22	95	41	28	16	-13
Europe	-38	-249	211	87	22	24	-171
Northern Africa	42	-85	128	27	-2	26	-9
Equatorial Africa	170	-151	322	89	13	103	-35
Southern Africa	79	-64	143	23	36	32	-11
Russia	17	-126	143	24	5	48	-61
Central Asia	-3	-3	0	5	-7	1	-2
Mideast	2	-48	50	37	1	1	-37
China	12	-106	118	23	4	28	-42
Korea and Japan	1	-16	17	3	1	1	-4
South Asia	44	-201	245	98	2	52	-108
Southeast Asia	237	-119	357	108	37	129	-36
Oceania	25	-29	53	36	1	9	-21

Table S2. Yearly mean E_{LUC} estimates of a BLUE simulation based on LUH2 at 0.25° resolution, 1960-2019, TgC*yr^{-1}).

	E_{LUC}	E_{SINK}	E_{SOURCE}	E_{CROP}	$E_{PASTURE}$	$E_{HARVEST}$	$E_{ABANDONMENT}$
Global	1563	-2591	4154	2263	237	635	-1572
USA	11	-186	197	51	2	36	-78
Canada	55	-55	110	28	1	34	-9
Central America	57	-97	155	111	10	20	-83
Northern South America	24	-64	88	61	15	7	-59
Brazil	356	-148	503	287	110	63	-104
Southwest South America	87	-56	143	104	10	17	-44
Europe	-57	-207	150	33	1	14	-106
Northern Africa	65	-164	229	117	1	25	-78
Equatorial Africa	191	-361	553	381	15	74	-279
Southern Africa	76	-178	254	150	11	29	-114
Russia	57	-210	267	44	0	75	-62
Central Asia	8	-7	15	11	1	1	-6
Mideast	10	-26	37	22	1	0	-13
China	171	-116	287	125	40	42	-36
Korea and Japan	-3	-23	19	3	1	1	-8
South Asia	96	-213	309	142	2	66	-114
Southeast Asia	269	-393	662	469	6	109	-315
Oceania	42	-20	62	42	3	8	-12

Table S3. Yearly mean E_{LUC} estimates of a BLUE simulation based on HILDA+ at 0.01° resolution, 1960-2019, TgC*yr^{-1}).

	E_{LUC}	E_{SINK}	E_{SOURCE}	E_{CROP}	$E_{PASTURE}$	$E_{HARVEST}$	$E_{ABANDONMENT}$
Global	986	-1394	2380	665	261	633	-573
USA	-29	-117	88	34	21	-4	-80
Canada	60	-53	113	11	1	57	-9
Central America	55	-25	80	33	13	21	-11
Northern South America	32	-13	45	6	20	13	-7
Brazil	203	-47	250	63	79	74	-13
Southwest South America	73	-21	94	40	28	17	-12
Europe	-40	-210	170	52	15	19	-126
Northern Africa	42	-84	126	26	-2	26	-8
Equatorial Africa	168	-146	314	83	12	103	-31
Southern Africa	79	-63	141	22	35	32	-11
Russia	17	-120	137	19	5	48	-55
Central Asia	-3	-3	0	5	-7	1	-2
Mideast	1	-37	39	25	1	1	-26
China	12	-104	116	21	2	28	-39
Korea and Japan	1	-15	16	3	0	1	-3
South Asia	46	-181	228	80	1	52	-86
Southeast Asia	227	-113	340	98	31	128	-30
Oceania	24	-24	48	32	-1	9	-16

E ELUC estimates based on HILDA+ and LUH2 over time

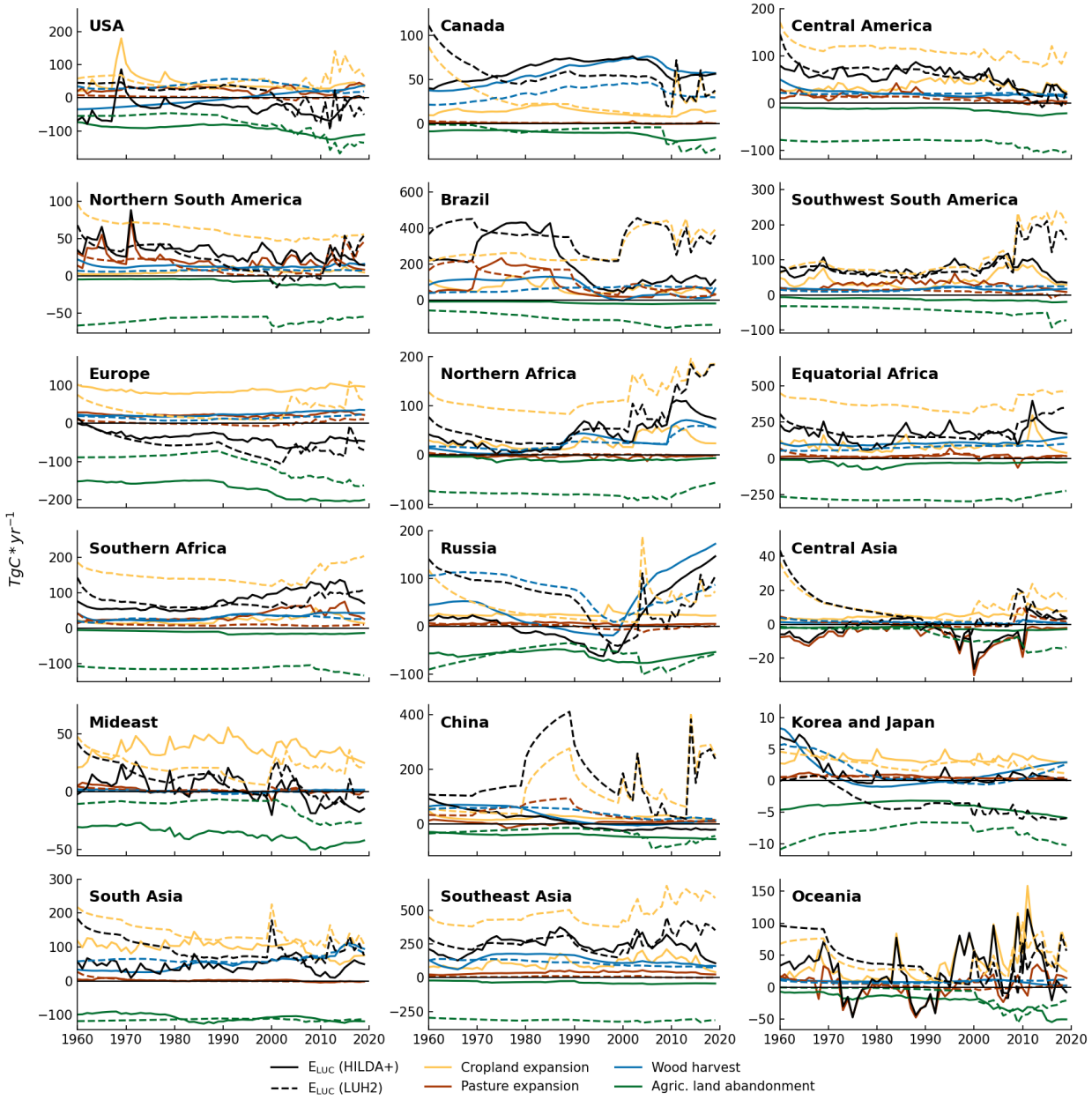

Figure S5. Net CO_2 fluxes from land-use and land-cover change (E_{LUC}) estimates based on HILDA+ and LUH2 (both at 0.25° resolution) of 18 regions.

F ELUC estimates based on HILDA+ at 0.25° and 0.01° resolution over time

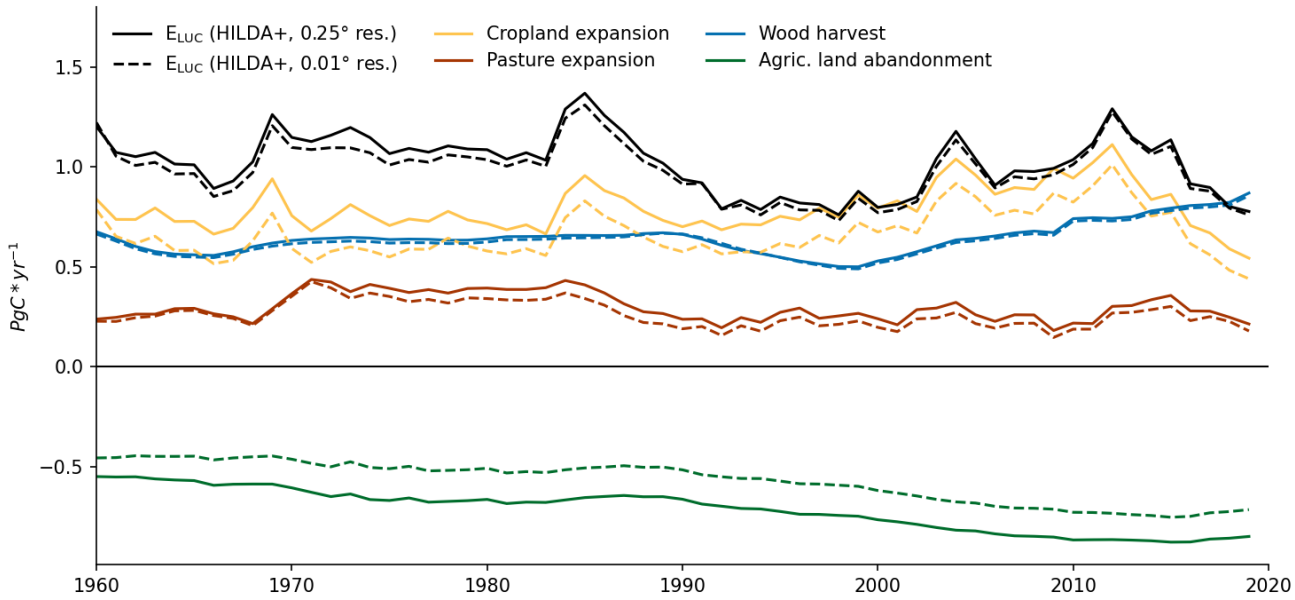

Figure S6. Global net CO_2 fluxes from land-use and land-cover change (E_{LUC}) estimates based on HILDA+ at 0.25° and 0.01° resolution.

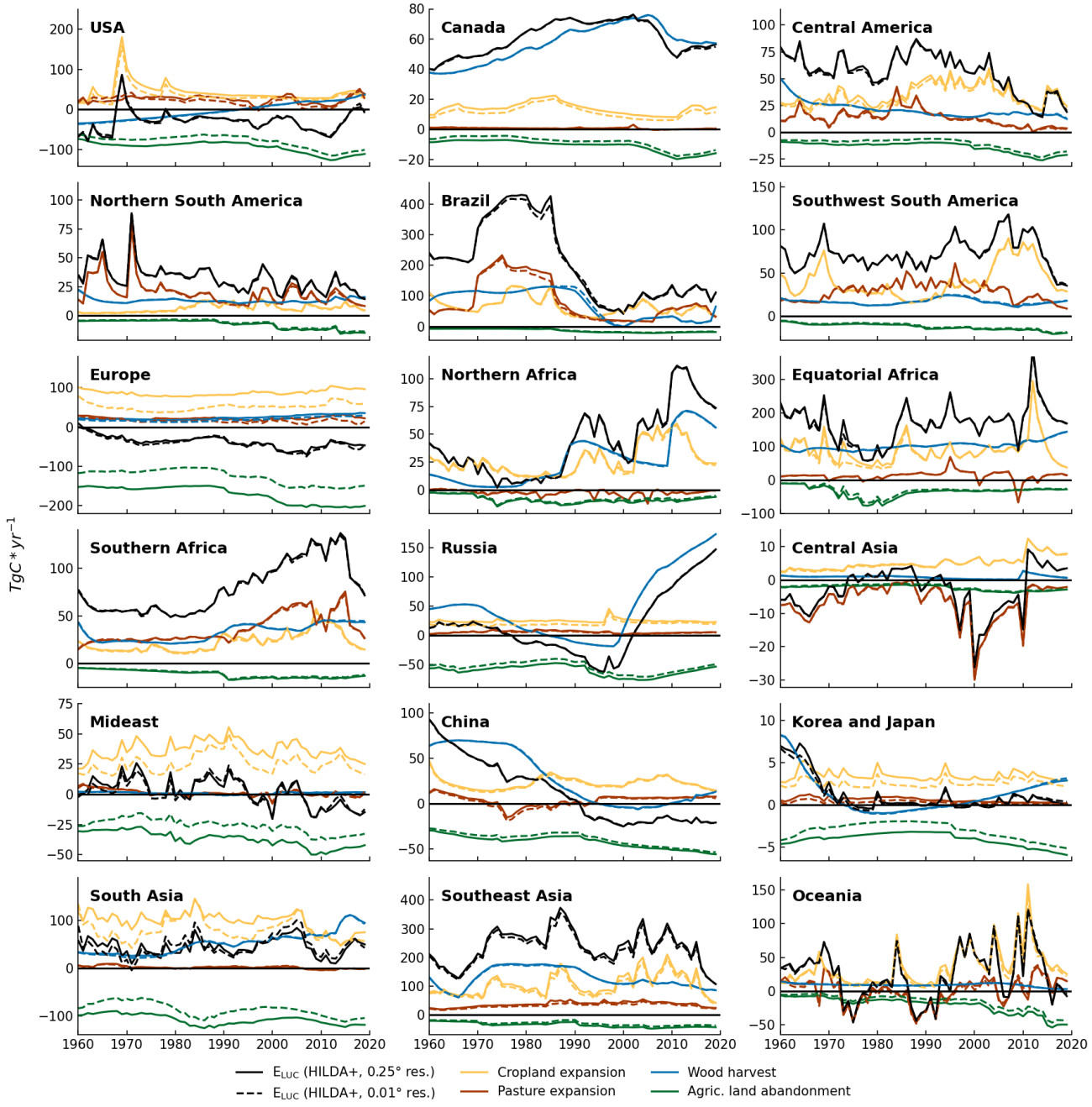

Figure S7. Net CO_2 fluxes from land-use and land-cover change (E_{LUC}) estimates based on HILDA+ at 0.25° and 0.01° resolution of 18 regions.

G Effect of successive transitions

To examine the observed differences between simulations at 0.01° and 0.25° resolution in more depth, we designed BLUE experiments with artificial LULCC input data. The extent of the experiment area is set to 0.25°x0.25°, which translates to 625 grid cells at 0.01° resolution and one grid cell at 0.25° resolution. Following the processing of the original HILDA+ data, the LULCC data at 0.25° resolution is created through regridding (method: conservative) of the 0.01° resolution data. The regridding method ensures that areas (e.g. states or transition areas) remain the same. The length of the simulations is limited to 100 years, the potential natural vegetation is set to be "Tropical evergreen forest" and the cover type at the beginning of the simulations is secondary land. For the experiments, we allow for three types of LULCC events. First, on the same 100 grid cells at 0.01°, which is about 16 % of the experiment area, transitions from secondary land to cropland happen in the years 10, 30, 50, and 70. For the simulation at 0.25deg, 16 % of the grid cell undergoes the transition from secondary land to cropland. Second, the same 100 grid cells experience the reverse transition from cropland to secondary land in the years 20, 40, 60, and 80. Third, on 100 different grid cells (no transitions) at 0.01° resolution, the wood harvest area is set to 50 % every year in the first 25 years. From this, we build three scenarios: (1) only transitions (secondary land to cropland and back), (2) only wood harvest, (3) transitions and wood harvest.

The results of the simulations are illustrated in Figure S8. At Scenario 1, emissions from the first transitions from secondary land to cropland and back (year 10 and 20) are the same at the two resolutions. However, emission fluxes differ significantly after the following transitions. While cropland emissions of the three later secondary land to cropland transitions are low and in each case the same level at 0.01° resolution, they are comparably high and slightly decreasing with each transition at 0.25° resolution. Similar, at 0.01° resolution the carbon uptake is always the same after the cropland to secondary transitions, whereas at 0.25° resolution it increases slightly with each abandonment event. Scenario 1 at 0.01° resolution shows that with each of the later secondary land to cropland transitions, the carbon stored in the previous 10 years without LULCC event is released. At 0.25°, the higher cropland emissions and higher carbon sink reflect how carbon pools of secondary land and crop are affected proportionally by LULCC events. In other words, at 0.25° resolution it can not be distinguished whether the secondary land to cropland transitions at year 30, 50, and 70 take place on the undisturbed area or the area, which was affected by the transition in year 10 and thus, a proportional influence is assumed.

Scenario 2 only considers harvest. At 0.01° resolution, it can be seen that the carbon stocks to harvest in the 100 grid cells affected by harvest, are depleted after around ten years. Following the harvest stop in year 25, the emission net flux from harvest turns negative, reflecting regrowth. At 0.25° resolution, emissions from harvest are larger in the 25 years but also decline over time, indicating decreasing carbon stocks in the 0.25° grid cell. Consequently, the carbon uptake is larger once harvesting stops. The peak at 0.25° resolution is caused by delayed emissions through decay. A comparison of the two simulations of Scenario 2 shows that more undisturbed area is affected by the annual harvesting events in the first 25 years at 0.25° resolution, while at 0.01° resolution the area where harvest can take place is more limited.

Scenario 3 is the combination of the first two scenarios and considers both transitions and harvesting events. At 0.01° resolution, Scenario 3 has the exact same net changes of cropland expansion and abandonment as Scenario 1 and harvest as Scenario 2, showing no reciprocal effects between transitions and harvest. This is logical, since lateral interactions between grid cells are not considered in BLUE and the 100 grid cells with transitions are spatially distant to the ones with harvest. In contrast, the interplay of transitions and harvest is apparent at 0.25° resolution. Here, the harvesting leads to far fewer emissions from the secondary land to cropland transitions. Especially, emissions from the first two secondary land to cropland transitions are significant lower compared to the estimates at Scenario 1 at the same resolution. After the harvesting stop in year 25, emissions from the secondary land to cropland transitions in year 50 and 70 adjust to the estimates of Scenario 1 at 0.25° resolution.

The experiments with artificial LULCC data highlight the sensitivity caused by the resolution for E_{LUC} estimates. The simulations show that (1) at different resolutions emission estimates are the same after the first LULCC event but differ after subsequent events; (2) component fluxes are higher at coarser resolutions compared to estimates at a finer resolution; (3) at lower resolutions successive LULCC events influence the E_{LUC} effect of every subsequent event, whereas at higher resolution the same LULCC events may be spatially separated and thus may not have an successive character.

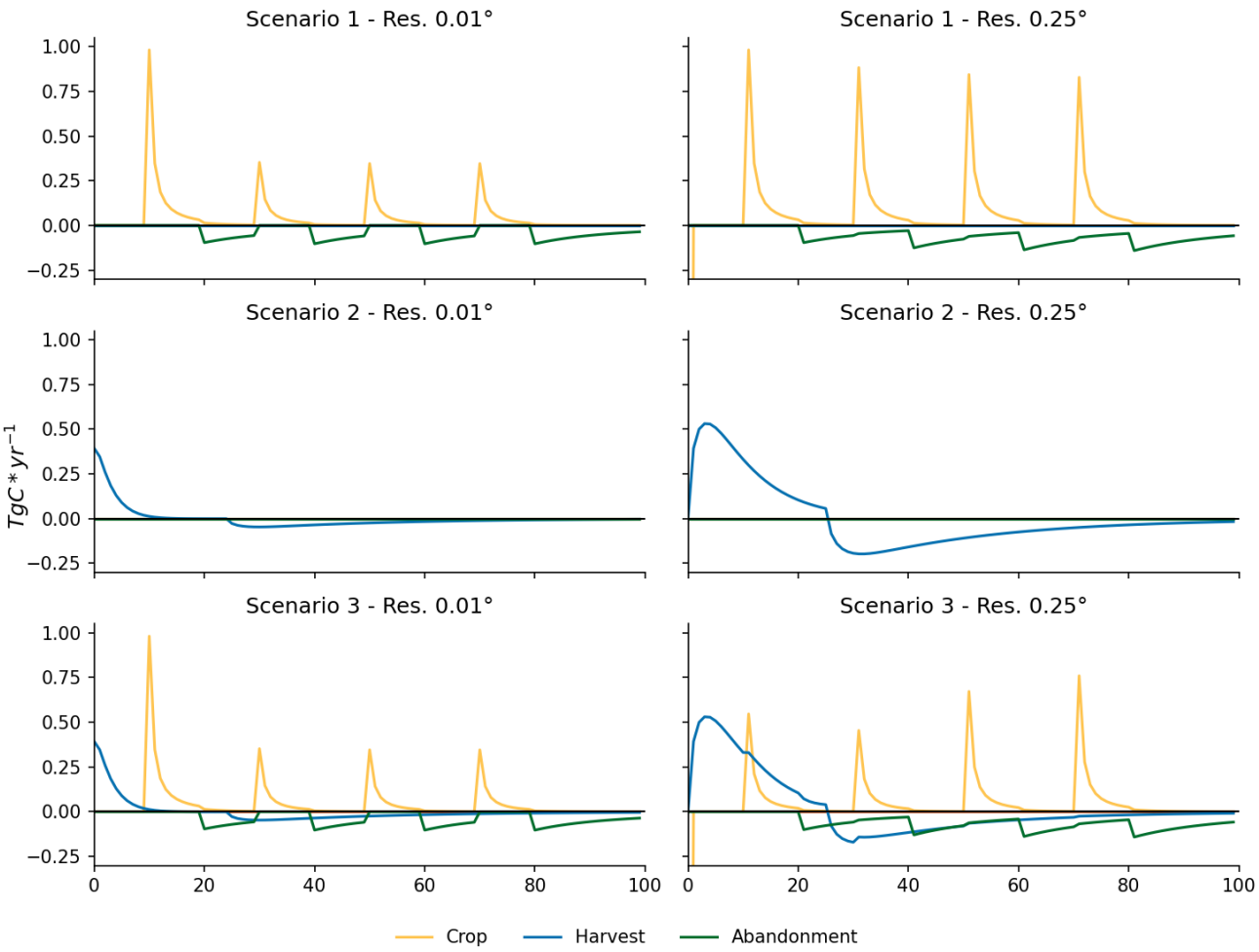

Figure S8. Net CO_2 fluxes from land-use and land-cover change (E_{LUC}) estimates based on artificial land-use and land-cover input data at 0.25° and 0.01° resolution. In scenario 1 only transitions but no harvest is considered, whereas scenario 2 includes only harvest and no transitions. Scenario 3 considers both transitions and harvest.

H Transitions in regions

Table S4. Average number of transitions in grid cells in prepared and reclassified HILDA+ dataset between 1900 and 2019 (%). The preparation of HILDA+ is described in Section 2. Globally, 84 % of the grid cells had no transition, 10 % had one transition, 5 % had 2-5 transitions and 1 % had more than 5 transitions in above-mentioned time period. For the resolution dependent "successive transitions" (Section 3.3), grid cells with more than one transition are of importance. Regions with a substantial amount of grid cells with successive transitions are Oceania, Europe, South Asia and Mideast.

	0 t.	**1 t.**	**2-5 t.**	**6+ t.**
Global	84	10	4	1
USA	79	11	7	2
Canada	98	1	1	0
Central America	82	13	4	1
Northern South America	88	8	4	0
Brazil	79	18	2	0
Southwest South America	79	17	4	0
Europe	68	11	13	8
Northern Africa	90	8	2	0
Equatorial Africa	81	14	4	1
Southern Africa	82	15	3	0
Russia	95	4	1	0
Central Asia	84	13	3	0
Mideast	83	9	5	2
China	73	24	2	0
Korea and Japan	88	9	3	0
South Asia	75	10	11	4
Southeast Asia	83	12	4	1
Oceania	37	29	29	5

I ELUC estimates based on LUH2 with different years of initialization

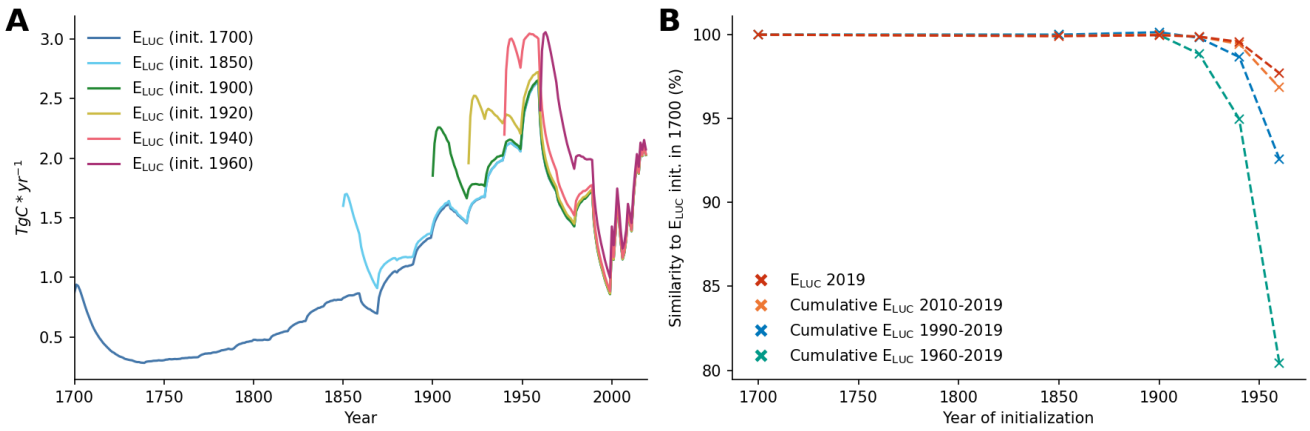

Figure S9. Comparison of BLUE runs with different initialization years based on LUH2 (res. 0.25°). Equivalent to Figure 5 with additional runs initialized in 1700 and 1850.

References

Chini, L. et al. (2021). “Land-Use Harmonization Datasets for Annual Global Carbon Budgets”. In: *Earth System Science Data Discussions*, pp. 1–27.

ESA (2017). *Land Cover CCI Product User Guide V. 2*. [Online; accessed 21. May 2021].

FAO (2021). *FAOSTAT*. [Online; accessed 21. May 2021].

Friedl, M. A. et al. (2002). “Global land cover mapping from MODIS: algorithms and early results”. In: *Remote Sensing of Environment* 83.1, pp. 287–302.

Hansen, M. C. et al. (2013). “High-Resolution Global Maps of 21st-Century Forest Cover Change”. In: *Science* 342.6160, pp. 850–853.

Heinimann, A. et al. (2017). “A global view of shifting cultivation: Recent, current, and future extent”. In: *PLOS ONE* 12.9, e0184479.

Hurtt, G. et al. (2020). “Harmonization of Global Land-Use Change and Management for the Period 850–2100 (LUH2) for CMIP6”. In: *Geoscientific Model Development Discussions*, pp. 1–65.

Klein Goldewijk, K., A. Beusen, J. Doelman, and E. Stehfest (2017). “Anthropogenic land use estimates for the Holocene – HYDE 3.2”. In: *Earth System Science Data* 9.2, pp. 927–953.

Le Quéré, C. et al. (2018). “Global Carbon Budget 2018”. In: *Earth System Science Data* 10.4, pp. 2141–2194.

Liu, H., P. Gong, J. Wang, N. Clinton, Y. Bai, and S. Liang (2020). “Annual dynamics of global land cover and its long-term changes from 1982 to 2015”. In: *Earth System Science Data* 12.2, pp. 1217–1243.

Pongratz, J., C. Reick, T. Raddatz, and M. Claussen (Sept. 2008). “A reconstruction of global agricultural areas and land cover for the last millennium”. In: *Global Biogeochemical Cycles* 22.3.

Ramankutty, N. and J. A. Foley (1999). “Estimating historical changes in global land cover: Croplands from 1700 to 1992”. In: *Global Biogeochemical Cycles* 13.4, pp. 997–1027.

Winkler, K., R. Fuchs, M. Rounsevell, and M. Herold (2021). “Global land use changes are four times greater than previously estimated”. In: *Nature Communications* 12.2501, pp. 1–10.

Zhang, X., E. A. Davidson, D. L. Mauzerall, T. D. Searchinger, P. Dumas, and Y. Shen (2015). “Managing nitrogen for sustainable development”. In: *Nature* 528.7580, pp. 51–59.